



3-1-9

ANALYSIS OF THE JMA STRONG-MOTION RECORDS FROM THE VIEWPOINT OF A POINT SOURCE MODEL

Ryosuke INOUE

Department of Construction Engineering, Ibaraki University,
Hitachi-shi, Ibaraki-ken, Japan

SUMMARY

We digitized the JMA strong-motion records (352 components) from 9 large earthquakes around the Japan arcs in order to investigate the characteristics of ground motions in the period of 2 to 20 sec, and analysed about a hundred components of them from the viewpoint of a point source model. First, we made a regression analysis of the velocity response spectra S_v using the records from four large events. However, the difference between the predicted S_v and the actual one were very large (as much as a factor of 5). Second, we analysed the records from 1983 Akita-Oki event and its largest aftershock in order to study whether the spectral ratio (main shock/aftershock) is independent of the station or not. The standard deviations of the ratio were very large (as much as the average values), and this suggests that we cannot disregard the difference between the paths of the two events. Third, we analysed the 1987 Chiba-ken-Oki event in order to investigate the relation between radiation pattern and characteristics of ground motions. We found that it strongly affect the initial motion of body waves at the stations with hypocentral distances of about a hundred kilometers, but has almost no influence on the spectra obtained from total ground motions.

INTRODUCTION

Investigation of the characteristics of ground motions in the period of 2 to 20 sec from large earthquakes is becoming increasingly important for aseismic design of large-scale structures (Ref.1). In this study, we digitized and processed 121 seismograms (352 components) from 9 earthquakes ($M_J=6.7\sim 7.9$) around the Japan arcs recorded by the JMA low-magnification seismograph network (JMA means the Japan Meteorological Agency) and analysed them from the viewpoint of a point source model.

JMA RECORDS AND OUTLINE OF THE ANALYSES

Table 1 shows the parameters of JMA strong-motion seismometer. Because of the limitations of its dynamic range and paper speed, it is suited for grasping roughly the characteristics of ground motions in the period of 2 to 20 sec. Table 2 is the list of digitized data, and Figure 1 shows the location of epicenters and JMA stations.

The digitized data were corrected for instrument characteristics, and the high and low frequency noise was removed by a bandpass filter (passband =2~20sec). The absolute time of the first data point in each record was determined (within a half second accuracy) from the time mark of the seismograph in order to study them seismologically.

We attempted to investigate the following three theme using the records from event 2,3,4,6,7,8 and 9. First of all, we made a regression analysis of the velocity response spectra (S_v with damping h of 0.1 and 2%) obtained from the records of event 2,3,4 and 6 ($M_j=6.7\sim 7.9$) using the parameters of G-R point source model (point source with scalar magnitude; Ref.2) as predictor variables. However, the discrepancy between the predicted S_v and actual one were very large (as much as a factor of 5; See Abstract). This discrepancy is probably due to the inadequate parameters of source, path and site we adopted in this analysis. Second, we analysed the records from Akita-Oki event and its largest aftershock (event 7 and 8; $M_j=7.7, 7.1$) from the viewpoint of the point source model in order to investigate whether the spectral ratio (main shock/aftershock) is independent of the station or not. In this analysis, we also used the GDSN records (GDSN means Global Digital Seismograph Network; Refs.3,4). Third, we analysed the records from Chiba-ken-Oki event from the viewpoint of double-couple point source model (Ref.6) in order to investigate the relation between the radiation pattern and characteristics of ground motions. We describe the results of theme 2 and 3 in some detail in the following sections.

ANALYSIS OF THE RECORDS FROM AKITA-OKI EVENT

We used the GDSN records from 9 stations (Fig.2) and JMA records from 5 stations (No.2,18,67,68,87 in Fig.1) in this analysis. In analysing the records we made the following assumptions: (1)Source region can be regarded as a point; (2)the system from the source to the station is linear; (3)the location of epicenter and focal mechanism of main shock are about the same as those of aftershock. From assumptions (1) and (2) we can write the ground motion $U(\omega)$ as

$$U(\omega) = \sum S_j(\omega) \cdot M_j(\omega) \cdot R_j(\omega) \quad (1)$$

where j is the index of each seismic ray and S_j, M_j, R_j are a source, medium and receiver function, respectively. If we further assume the source as a point double-couple, we can write the source function as

$$S_j(\omega) = Mo(\omega) \cdot (Rad)^{\circ}_j / (4\pi \rho c^3) \quad (2)$$

where Mo and $(Rad)^{\circ}_j$ are a moment rate function and radiation pattern, respectively. (Refs.4,6,9). Following Eqs.(1),(2) and assumption (3), we can write the spectral ratio (main shock/aftershock) as

$$U(\omega)/u(\omega) = Mo(\omega)/mo(\omega) \quad (3)$$

where u and mo are parameters of the aftershock. From this formula, we can see that the ratio should be station independent.

As the time window T_w for computing Fourier spectra, we adopted the portion of P waves for GDSN records (Fig.3 and Ref.5) and that of body waves for JMA records. From Figure 4 the following can be seen: (1)The average spectral ratio of GDSN stations is about two or three times larger than that of JMA; (2)the standard deviations of the ratio are very large (as much as the average values). These results are probably due to the complexities of natural phenomena, and suggest that we cannot disregard the difference between the location of hypocenter of the main shock and that of the aftershock (difference between the paths of the two events).

ANALYSIS OF THE RECORDS FROM CHIBAKEN-OKI EVENT

Figure 5 shows the locations of epicenter and JMA stations, and Figure 6 shows the distribution of the initial compression-dilatation of P waves. From Figure 6 and the distribution of the aftershocks, we deduced the fault plane and slip vector as shown in Fig.7 by the method described in Ref.7. We used the formula (4)~(6) for the interpretation of the records (Fig.8 and Refs.8,9,10), where we ignore the anelastic attenuation for the sake of simplicity.

$$U^P(t) = \dot{M}_p(t-T_p) \cdot (Co)^P, \quad U^{SU}(t) = \dot{M}_p(t-T_s) \cdot (Co)^{SU}, \quad U^{SH}(t) = \dot{M}_p(t-T_s) \cdot (Co)^{SH} \quad (4)$$

where

$$\begin{aligned} (Co)^P &= R(i_h, \phi_s) \cdot C_p / r, & (Co)^{SU} &= R(i_h, \phi_s) \cdot C_{SU} \cdot (\alpha/\beta)^3 / r, \\ (Co)^{SH} &= R(i_h, \phi_s) \cdot C_{SH} \cdot (\alpha/\beta)^3 / r \end{aligned} \quad (5)$$

(C_p, C_{SU} and C_{SH} are 'free surface effect' (~2); Refs.8,9,10)

and

$$\dot{M}_p(t) = \dot{M}_o(t) / (4\pi \rho \alpha^3) \quad (6)$$

In these formulas, we call Co 'amplitude coefficient' (Table 3), and \dot{M}_p 'moment rate factor', respectively.

Figure 9 shows the example of $M_o(t)$ and corresponding ground motion. From definition of M_o , it follows that

$$\int \dot{M}_o(t) dt = M_o \quad (M_o; \text{ seismic moment}) \quad (7)$$

From Eqs.(4)~(7) we can see that the area of the pulse of the initial motion of body waves is proportional to $M_o \cdot (Co)$ and is independent of the pulse shape.

Figure 10 shows an example of ground displacement. In this figure, the arrows indicate the beginning of P and S waves determined from the JMA standard travel-time tables (Ref.11), and the hatched portions are the areas from which we determined M_o . Table 4 shows the estimated value of seismic moment obtained from the records with a hypocentral distance (r) of about a hundred kilometers. The average value ($\sim 2 \times 10^{26}$ dyne·cm) nearly coincide with the experimental value ($\sim 1.1 \times 10^{26}$) obtained from the next formula (Ref.12).

$$\log_{10} M_o = 1.5 \cdot M_j + 16 \quad (8)$$

This coincidence and relatively small variances of the values between each component (within a factor of 2) compared with that of Co (Table 3) strongly suggest that the radiation pattern have a great influence on the initial motion of body waves at the stations with $r \approx 100$ km. Figure 11 shows the Fourier amplitude spectra of ground acceleration (time window =90 sec) obtained from the stations situated in the loop direction of SH-wave (with large $(Co)^{SH}$; Fig.6 and Table 3). In this Figure, there is no systematic difference between the values of spectra of transverse component and those of the radial component, and this suggests that the radiation pattern has almost no effect on the spectra obtained from the total ground motions (probably due to the scattering of waves in the heterogeneous medium).

REFERENCES

1. Inoue, R., "Studies on Design Earthquakes in the Period Range of 2 to 20 sec - A Review (In Japanese)," Proceedings of JSCE, No.374/1-6, 1-23, (1986).
2. Gutenberg, B. and Richter, C.F., "Earthquake Magnitude, Intensity, Energy and Accelerations", Bull. Seism. Soc. Am., 32, 163-191, 1942.
3. Engdahl, E.R., Peterson, J. and Orsini, N.A., "Global Digital Networks - Current Status and Future Directions," Bull. Seism. Soc. Am., 72, 243-260, (1982).
4. Houston, H. and Kanamori, H., "Seismic Spectra of Great Earthquakes: Teleseismic

- Constraints on Rupture Process and Strong Motion," Bull. Seism. Soc. Am., 76, 19-42, (1986).
5. Jeffreys, H. and Bullen, K.E., Seismological Tables, British Association for the Advancement of Science, Gray-Milne Trust, Neil & Co. Ltd., Edinburgh, (1940).
 6. Honda, H., "The Mechanism of Earthquakes," Science Reports, Tohoku University, Series 5, Geophysics 9, 1-46, (1957).
 7. Kasahara, K., Earthquake Mechanics (In Japanese), Kajima Institute Publishing Co. Ltd., (1983).
 8. Kanamori, H. and Stewart, G.S., "Mode of the Strain Release along the Gibbs Fracture Zone, Mid-Atlantic Ridge", Phys. Earth Planet Int., 11, 312-332, (1976).
 9. Bullen, K.E., An Introduction to the Theory of Seismology, Cambridge University Press, (1965).
 10. Honda, H., Seismic Waves (In Japanese), Iwanami, (1954).
 11. Japan Meteorological Agency, A Guide to Seismic Observation (Volume of Analysis; In Japanese), 94-124, (1971).
 12. Kasahara, K., "Standard Values of Fault Parameters (In Japanese)", Abstract of Seism. Soc. Japan, 2, p.8, (1975).

ACKNOWLEDGMENTS

We would like to thank all the JMA stations that were kind enough to send us seismograms for the events used in this study. We would also like to thank Prof. Kanamori and Dr. Houston (Caltech) who provided us with the computer programs for analysing GDSN records. Prof. Seo and Dr. Kitagawa are thanked for suggesting us to analyse the records of Chiba-ken-Oki event and Y. Sakuma (JMA) kindly provided us the materials for the event. We are grateful to H. Takahashi and others for digitizing those records and Prof. Fujino for his encouragement. This research was supported by the Science Research Fund of the Ministry of Education of Japan.

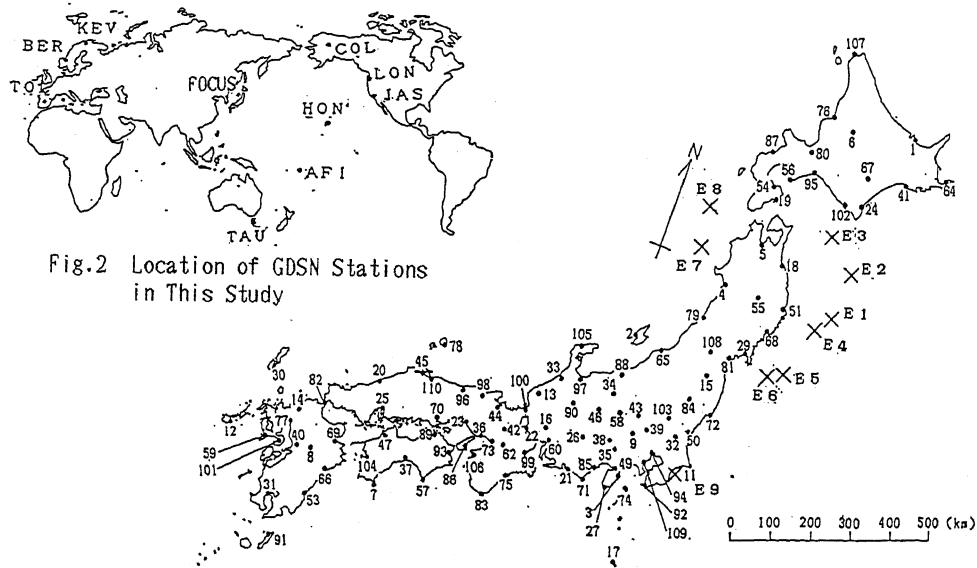


Fig.1 Location of Epicenters (E1~E9) and JMA Stations (Total 111)

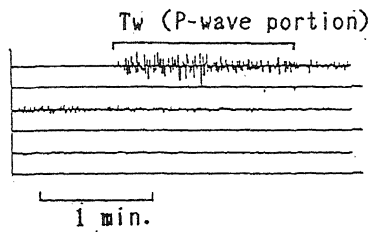


Fig.3 Example of GDSN Records
(Main Shock, KEV, UD-Comp.)

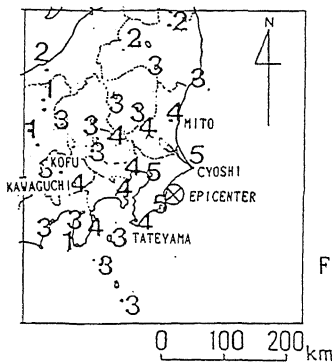


Fig.5 Location of Epicenter and JMA Stations

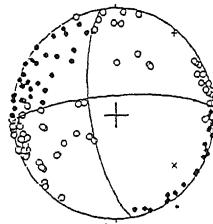


Fig.6 Equal-Area Projection of the P-Wave First-Motion (Upper Hemisphere) (Data: JMA, NRCDP) (●: Compression) (○: Dilatation)

Fig.7 Inferred Fault Plane and Slip Vector (Right)

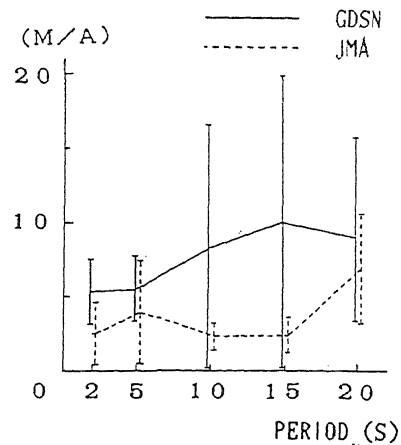
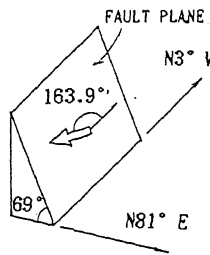


Fig.4 Average Spectral Ratio (Main Shock/Aftershock) (Vertical bars show standard deviations)

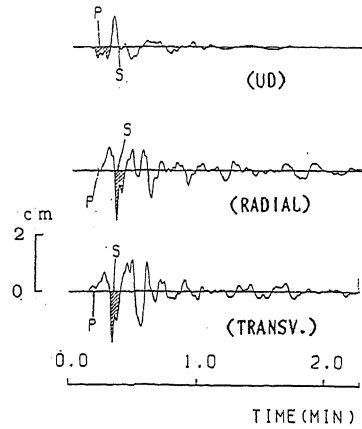


Fig.10 Example of Ground Displacement (CYOSHI)

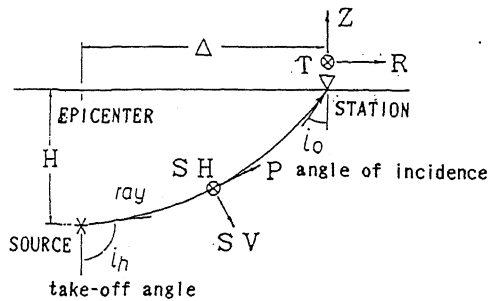


Fig.8 Schematic Diagram of the Propagation of the Direct Body Waves

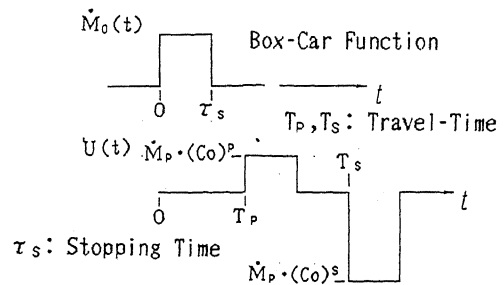


Fig.9 Schematic Diagram of Moment Rate Function (Above) and Theoretical Ground Displacement (Below)

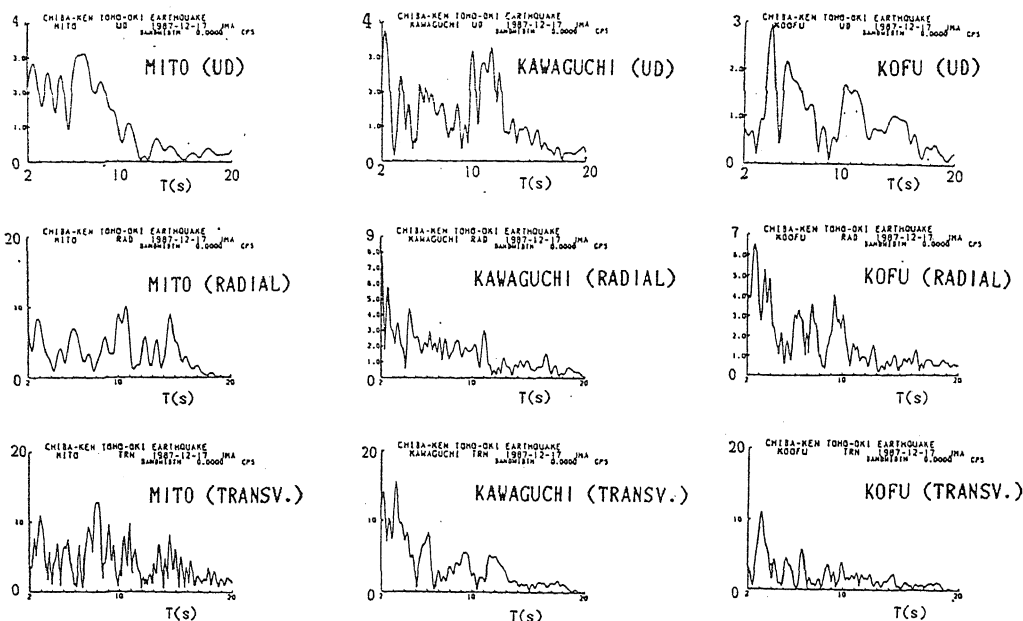


Fig.11 Fourier Amplitude Spectra of Ground Acceleration
for the Time Interval of 90 sec (gal·sec)
(These stations are in the loop direction of SH waves)

Table 1 Instrumental Characteristics of
JMA Strong Motion Seismometer

Type : Mechanical Seismometer
Free Pendulum Period: 6s(H), 5s(V)
Damping Coefficient : 0.5519
Statical Magnification: 1
Maximum Amplitude of the Record: 3 cm
Dynamic Range: ~100
Paper Speed : 0.5 mm/sec

Table 2 List of Digitized Data

No.	Name	Date	M	D	N of (km) Comp.
E1	Sanriku-Oki	1960. 3.21	7.5	20	31
E2	Tokachi-Oki	1968. 5.16	7.9	9	47
E3	(Aftershock)	1968. 5.16	7.5	26	39
E4	(Aftershock)	1968. 6.12	7.2	31	38
E5	Miyagi-Oki	1978. 2.20	6.7	50	16
E6	Miyagi-Oki	1978. 6.12	7.4	48	57
E7	Akita-Oki	1983. 5.26	7.7	14	56
E8	(Aftershock)	1983. 6.21	7.1	6	42
E9	Chibaken-Oki	1987.12.17	6.7	58	26

Table 3 Amplitude Coefficient (Co)
of the Direct Body Waves

Station	r (km)	ϕ_s (deg)	(Co) ^{PZ} ($\times 1/100$)	(Co) ^{SU} (1/km)	(Co) ^{SH} (1/km)
CYOSI	78.6	38.3	-1.3	-6.9	-3.2
TATEYAMA	90.1	234	-1.2	-4.9	-1.9
MITO	128	0	-0.63	1.1	6.4
KAWAGUCHI	167	277	0.25	1.6	-4.9
KOFU	187	282	0.40	1.6	-4.0

(r: hypocentral distance, ϕ_s : station azimuth
measured clockwise from the north)

Total 352

Table 4 Estimated Value of
Seismic Moment

Station	UD	RAD.	TRNS.	AV.
CYOSHI	2.0	1.0	1.7	1.6
TATEYAMA	2.2	2.1	3.2	2.5
MITO	-	-	-	2.6

($\times 10^{26}$ dyne·cm)